Influence of the Paste Composition On the Rheological Properties of the Ceramic Screen-Printing Inks

Anna Kolesova

Keywords: rheology, screen-printing, ceramic, paste

1. Introduction

Paste technology is an economically beneficial manufacturing method, which maximizes the product output and minimizes waste and emissions. It can be used for different applications. Paste technologies are often employed together with the printing and coating technologies.

One of such method is screen- printing, which is considered as one of the most convenient and simplest printing techniques. In the screen-printing process, the paste is transferred on the substrate through the stencil, which is a water and solvent resistant coated screen. Screen- printing is an old, but until now very widely used printing technique due to its practicality. There are several benefits in this printing process such as flexibility of the process and possibility to use huge variety of substrates, inks and pastes. The screen- printing method is often employed for printing parts of energy source devices.

The material of the screen mesh (e.g., PET or metal threads), mesh count (the measure of number of threads per square inch), mesh opening (the distance between two adjacent warps) and mesh thickness determine the percentage of open area and total ink volume to be transferred through the meshes on the substrate. Hence, the screen mesh characteristics regulate the thickness of the printed layer and the minimum possible thickness of the printed line. The higher the mesh count, the finer the lines, that can be achieved [18].

Robert Bosch GmbH Electrochemical Material Technologies (CR/ATC3)

Consequently, the printing quality depends on the screen type, printer settings, materials, and ink rheology. Most of those parameters can be adjusted and controlled during the process of printing except the ink rheology [3]. Therefore, to optimize the screen-printing process, the rheological parameters of the printing inks must be analyzed and regulated before the printing process starts. Several factors influence the rheological parameters of the pastes such as type of the composites and their chemical and mechanical properties, composition of the pastes, meaning the amount of each variable in a system, and the temperature. In this work, the influence of the paste composition on rheological properties is evaluated. The data analysis is done by a design of experiment program (DoE), called Cornerstone. The correlation between the factors such as binder, solid and powder content on rheology factors is evaluated. The analyzed rheology factors in this case are shear viscosity, complex viscosity and loss factor.

2. Screen-printing Paste

Screen- printing paste consists of organic and solid phases. Powder plays a functional role in the paste, based on the application and the requirements of the printed film. For example, in the field of printed electronics, solid particles, depending on their chemical properties, can either contribute to the conductivity of the film or on the other hand build an isolation layer. As for the color industry, the solid phase is a coloring pigment. The stabilization of the solid particles is provided by a variety of forces such as Van der Waals forces, electrostatic forces, liquid bridging (capillary) and repulsing forces [9]. Particle interactions are size dependent, such that small (between 1 nm and 0.1 micrometer) particles experience stronger colloidal interaction, resulting in an increase of the viscosity of the suspension due to stronger attraction and higher friction. A viscosity reduction within a sample can arise from mixing particles of different sizes or having only non-Brownian particles (larger than 10 micrometers) in a system [10].

The organic phase contains solvent, binder and additives. The main function of the binder is a fixation of the solid particles in liquid and dry phases. Solvent dissolves the binder agent and reduces the viscosity. Different additives can be added, depending on the required mechanical properties of the printed layer. For example, plasticizer increases the flexibility of the film after the drying process.

Rheological characteristics and the printability of the pastes are influenced by the powder properties such as specific surface area and particle size distribution. Type and content of added binder and additives also have a big impact on the paste properties and therefore on rheology and printing process.

3. Experimental Setup and Analytical Method

Cornerstone is a statistical program for the design of experiment, which is used to create the experimental setups and evaluate the influence of the sample composition on the rheological properties of the pastes.

The software works with the factors and responses and finds connection between them. The analyzed parameters such as binder, solid and plasticizer represent factors. The responses are the rheological values such us shear viscosity, complex viscosity and loss factor. The resultant outcome is a mathematical function, which links the factors and responses. The statistical analysis generates regressions, probability plots and dependency graphs, which will be explained in detail in chapter 4.6.

The experiment is created in a design space, which is defined by experimental parameters of the variables: their minimum and maximum values. The boundaries of each variable used in this work are presented in volume percent in Table 1.

Solid [Vol %]	Binder [Vol %]	Plasticizer [Vol %]
22-32	9-17	0-10

Table 1. *Minimum and maximum values for the composition of the samples.*

Within given design space, the set of samples is generated with the general goal of maximizing the amount of information gained from a limited number of samples [11]. The type of space design defines the way the set of samples are made.

In the current work, "space-filling" design of experiment has been used. Cornerstone uses Sobol sequence as a space filling design. Sobol sequence belongs to the family of quasi-random sequences, which are designed to generate samples of multiple parameters as uniformly as possible over the multi-dimensional parameter space [12]. Space-filling design avoids replicates and efficiently fills the gaps in a factor space. Compared with the "classical „or "D-optimal" designs, where the sample points are located on the boundaries, the sample points of the space- filling design are mostly spread in the middle of the range (Fig.1).

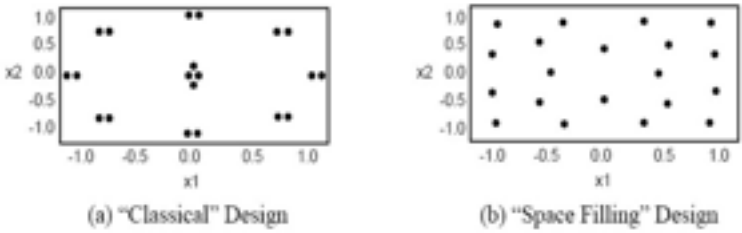

Figure 1. *Adapted from [13]: space designs.*

The set of samples, shown in the Table 2, has been generated by the Cornerstone and used for further steps: sample preparation and statistical analysis.

Sample	Solid [Vol-%]	Binder [Vol-%]	Plasticizer [Vol-%]	Solvent [Vol-%]
P595	25,75	12	6,25	56
P596	30,75	16	1,25	52
P597	22,63	16,5	5,63	55,24
P598	29,5	11	2,5	57
P599	26,38	13,5	1,88	58,24
P600	28,25	10	8,75	53
P601	25,44	14,75	7,19	52,62
P602	25,13	10,5	3,13	61,24
P603	24,5	15	7,5	53
P604	31,38	9,5	6,88	52,24
P605	27,94	16,75	9,69	45,62
P606	22,94	12,75	4,69	59,62
P607	30,13	14,5	8,13	47,24
P608	27,63	12,5	0,63	59,24
P609	23,25	14	3,75	59
P610	23,88	11,5	9,38	55,24
P611	27	13	5	55
P612	28,88	15,5	4,38	51,24
P613	30,44	10,75	2,19	56,62

Table 2. *Pastes composition, space-filling design of experiment.*

4. Samples Preparation

The paste compositions had to be calculated, using specific densities of all components for achieving the needed amount in g of all components ($V = m/\rho$). The samples were prepared under constant conditions in a clean room. The paste components were weighed in the right amount in a laboratory jar (Fig.2) and premixed by steering with a spatula, followed by mechanical premixing with a speed mixer (DAC 400 FVC).The deagglomeration of the powder was done in a triple roll mill Exakt 80E (Fig. 3). Speed of the rolls is set in a ratio of 3:6:9, what generates a shear force between the rolls [3]. All samples used for rheological tests, were of 5 ml volume. Twenty-four hours before the rheology test, the pastes were premixed in the speed mixer again. Rheological data was collected on a controlled shear stress rheometer MCR500 of Anton Paar GmbH at a constant temperature of 25°C.

Figure 2. *Laboratory jar and spatula.*

Figure 3. *Triple-roll mil.*

5. Rheology and Rheometry

Rheology plays a crucial role in the determination of the paste properties. It is defined as the study of the deformation of matter, resulting from the application of force. Using the rheological terms, the flow behavior of the material at rest or under applied stress can be described. The degree of deformation depends on the state of a substance. The sample in a solid state is deformed until certain extend and expected to be recovered after the force is removed, while liquids and gases flow under application of force with different speed [14]. Rheometry is an experimental technique, used to evaluate the rheological behavior.

Two-Plates Model can be used to describe the main rheological parameters. The bottom plate is fixed, while the upper plate with the area A moves parallel to the lower plate with the certain velocity v due to application of the shear force F. The gap between the plates is defined by the distance h. The sample, applied in the gap, gets in contact with both plates. Therefore, the fluid is set in motion due to the displacement of the upper plate (Fig.4).

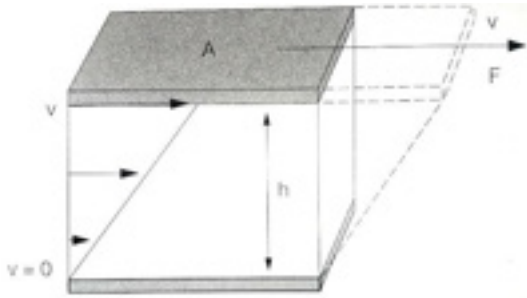

Figure 4. *Adapted from [16]: Two-Plate Model.*

Using Two-Plate Model, shear rate and shear stress are determined to calculate the shear viscosity. A ratio of velocity v and the distance h defines shear rate: $\dot{\gamma} = v / h$. Shear stress is defined by a ratio of shear force F and shear area A: $\tau = F / A$. Viscosity η is defined as shear stress t divided by shear rate γ: $\eta = \tau / \dot{\gamma}$. Shear viscosity can be described as a measure of the resistance to the flow. It is not a constant rheological parameter as viscosity of the sample changes under application of shear. Different shear behaviors can be evaluated through the rotational rheological tests.

5.1. Flow behaviors and rotational tests

Flow behavior depends on the sample. Therefore, several types of the flow behavior are differentiated and illustrated in Figure 5: Newtonian, Shear- thinning or Pseudoplastic and Shear- thickening or dilatant flow behaviors.

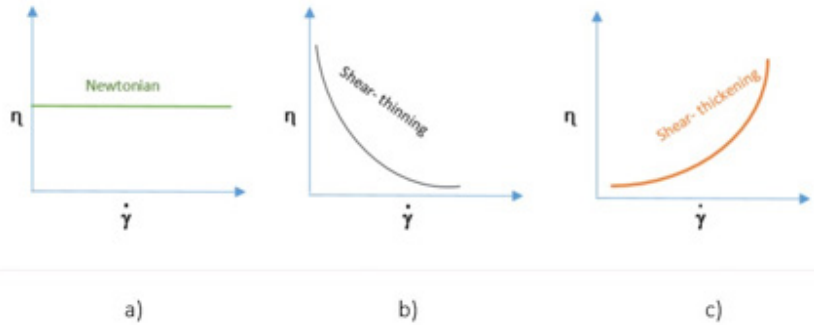

Figure 5. *Based on [16]: different flow behaviors.*

Ideal viscous or Newtonian flow behavior

Viscosity of such materials is constant and does not depend on the shear rate (Fig.5a). Examples of Newtonian fluids are water, mineral oil, silicon oil, salad oil, solvents such as acetone [16].

Shear-thinning flow behavior

Shear-thinning flow behavior or pseudoplastic flow behavior is characterized by decreasing viscosity with increasing shear rate (Fig 5b). Materials, which belong to this group, are coating, glue, shampoos, polymer solutions and polymer melts [16]. Shear- thinning behavior is an indicator of the printability of the pastes, as in screen- printing process, the decrease of viscosity due to the force exceeded by the squeegee results in homogeneous transfer of the pastes through the meshes onto the substrate [6].

Shear-thickening or dilatant flow behavior

Shear thickening or dilatant flow behavior is given as the viscosity increases with increasing shear rate (Fig 5c). Typical materials, which show this flow behavior: high filled dispersions, starch dispersions, plastisol pastes that lack plasticizer, dental filling masses [16]. In the screen-printing process the dilatant behavior of the pastes would lead to blockage of the meshes as the viscosity increases during the process stage.

Flow behavior is evaluated by the shear ramp up rotational test, where shear rate is constantly increasing and the viscosity curve is plotted at each shear rate value. Generally, rotational tests are carried out either to simulate force-dependent applications (e.g., force required to squeeze the paste through the meshes) or simulate the processes that are dependent on flow velocity (e.g., application of

coating by spraying) [16]. In both cases the structure of the sample is destroyed. Geometry of the rotation shear test is illustrated on Figure 6, where the lower plate stays still, and the upper cone rotates.

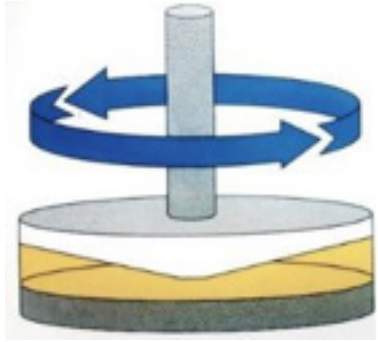

Figure 6: *Adapted from [16]: rotational shear test.*

5.2. Rheological parameters and oscillatory tests

Oscillation testing mode is used to analyze the sample in non-destructive or reversible deformation range. The basic principle of an oscillatory rheometer is to induce a sinusoidal shear deformation in the sample and measure the resultant stress response [15]. The sample with ideal elastic behavior shows immediate stress response as the strain and stress curves are identical, while viscoelastic materials experience the phase shift δ, which is always between 0° and 90°. The phase shift of fluids lays between 46° and 90°. Those dependencies are illustrated in Figure 7.

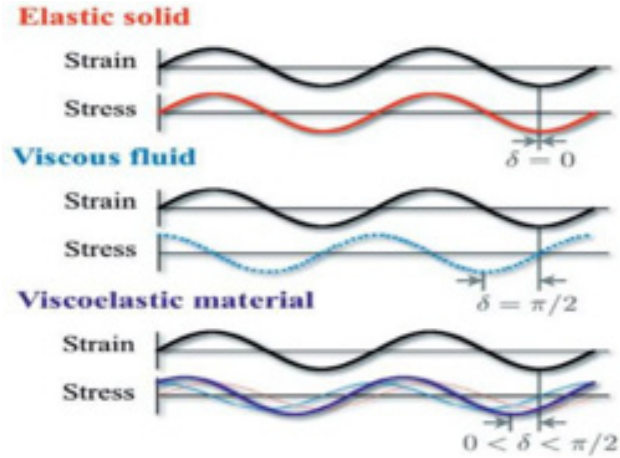

Figure 7. *Adapted from [15]: stress oscillation testing mode.*

Behavior of the paste at different states, for example, during storing, processing and recovery is evaluated by the oscillatory tests. In this work Amplitude-Sweep, Frequency-Sweep, Creep and Recovery oscillatory tests were carried out.

Amplitude Sweep Test

Amplitude-Sweep test must be executed first, to determine the linear- viscoelastic range (LVE). During the test, the amplitude is increasing while the frequency stays constant (Fig.8). If the sample is within LVE rage, the structure is not destroyed. If the upper limit exceeds due to increased amplitude, the structure either breaks down or softens. This phenomenon is presented by Figure 9, where the storage modulus G' represents the elastic portion in a sample, namely the deformation energy stored in a paste during the shear process [17]. After the removal of shear force, the energy is released and works upon the compensation of the preceding deformations. Materials, which tend to return to their original form show reversible deformation behavior. The loss modulus G" represents the viscous portion in a sample and the energy, which is lost due to the shear force. Consequently, samples with predominate G" value reveal irreversible deformation behavior.

In Figure 9, it can be seen at low deformation range (within LVE range), that storage modulus is bigger than the loss modulus (G' > G"), what indicates solid state of the sample within LVE range. Yield point τ_y shows the limit of LVE range, while the crossover (G'= G") τ_f (yield stress) represents the point, where the sample starts to flow. In this scenario, the viscous portion becomes dominant (G'< G") due to high deformation. This behavior is inherent in gels and viscoelastic solid.

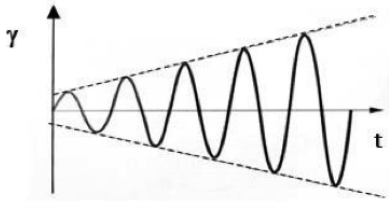

Figure 8. *Adapted from [16]: Amplitude sweep.*

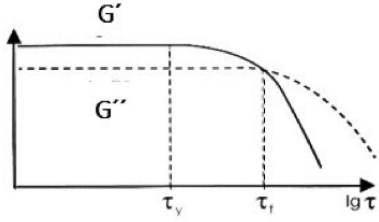

Figure 9. *Adapted from [16]: Limit of LVE region.*

On the other hand, fluid samples express dominant viscous behavior (G'< G") in the LVE range as shown on the Figure 10. In this case, the crossover point cannot be determined as the sample flows over the whole deformation range.

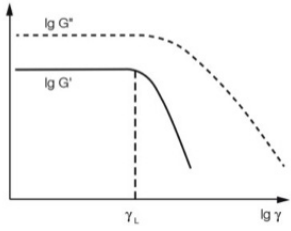

Figure 10. *Adapted from [16]: Limit of LVE range*

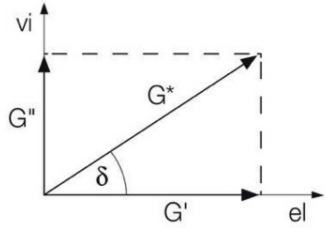

Figure 11. *Adapted from [16]: Vector diagram.*

The complex sum of two components G´ (on the x-axis) and G" (on the y-axis) is G* (complex shear modulus). The vector diagram of Figure 11 represents complex shear modulus using the phase shift angle δ.

Frequency-Sweep test

The Frequency-Sweep test is used to simulate fast motion on short time scale, whereas low frequencies simulate slow motions on long timescale. The test results describe the behavior of a sample in the non-destructive deformation range; therefor the LVE range has to be determined in advance by Amplitude- Sweep test [16]. During the test, the amplitude stays constant, only the frequency changes (Fig. 12).

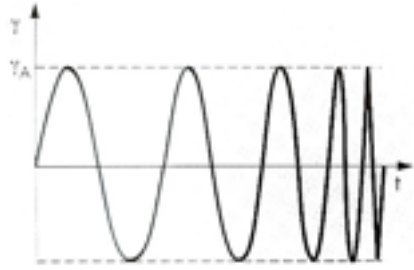

Figure 12. *Adapted from [17]: Frequency sweep.*

Step Test or Creep and Recovery Test

In this work, oscillatory Step test has been performed in three intervals to evaluate time- dependent structural regeneration of the samples. The experiment is comprised in three intervals. Resting interval (step 1), where very low shear rate is applied. Process interval (step 2), which simulates the deformation of the sample due the application of force by the squeegee during the screen-printing process and often corresponds to complete breakage of the inner structure of the material. Recovery interval (step 3), which refers to the time required for the structural regeneration. Figure 13 illustrates typical result of Creep and Recovery test, where complex viscosity is decreasing during the process step and completely recovers at the step 3.

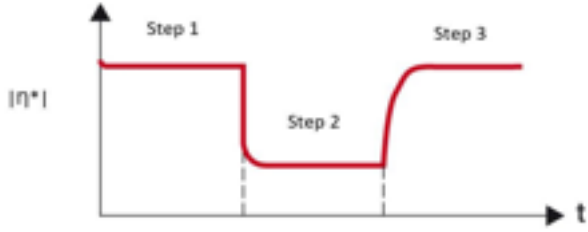

Figure 13. *Creep and Recovery test.*

Shear viscosity can be measured by rotational tests (see Figure 5), while the rheological parameters such as loss Factor tan d and complex viscosity η* are derived from oscillatory tests.

Loss Factor

Loss factor tan d is defined by the ratio of the viscous to the elastic portion of the deformation behavior [17]: tan δ = G" / G´. If the sample express ideally elastic behavior, the viscous portion is missing (G"=0). Therefore, the loss factor would be zero: tan δ = 0 = G" / G´. In contrary, the loss factor (tan δ) of the sample with ideal viscous behavior, where the elastic portion is missing (G´=0), will be approaching infinity due to the attempt to divide by zero. Generally, if the loss

factor is bigger than one (tan δ > 1), then the sample shows predominate viscous behavior. On the other hand, if the loss factor is lower than one - elastic behavior (tan δ < 1). Viscoelastic behavior is recognized when the loss factor does not equal to 0 or infinity.

Complex Viscosity

Complex viscosity is defined by the Newton´s law: $\eta^* = \tau(t) / \dot{\gamma}(t)$, where $\tau(t)$ and $\dot{\gamma}(t)$ are sinusoidal functions. The complex viscosity is measured in an oscillatory test and calculated by using complex numbers.

5.3. Sequences of the rheological tests

All samples were tested using two test profiles, which are presented in the tables below. Profile I includes the creep and recovery test, which is carried out in the segments 2-4 (Table 3). Segment 5 corresponds to the shear rate ramp up test, where the flow behaviour of the pastes with the increasing shear rate is evaluated. Profile II (table 4) includes Amplitude-Sweep test in segment 2 and Frequency-Sweep test in segment 3, followed by the rotational test with increasing shear rate.

Segment	Phase	Test parameters
1	Rest	-
2	Oscillation	γ: 0,2% ω: 10 rad/s
3	Oscillation	γ: 20% ω: 10 rad/s
4	Oscillation	γ: 0,2% ω:10 rad/s
5	Rotation	$\dot{\gamma}$: 0,1….50 1/s

Table 3. *Test profile I*

Segment	Phase	Test parameters
1	Rest	-
2	Oscillation	γ: 0,001..20% f: 1Hz
3	Oscillation	γ: 0,05% f: 100….0,1Hz
4	Rotation	$\dot{\gamma}$: 0,1….10 1/s
5	Rotation	$\dot{\gamma}$: 1….1000 1/s

Table 4. *Test profile II*

6. Results and Evaluations

The solid phase of the tested samples is a ceramic powder of spherical shape. The mean particle size is ~ 0,2 µm and the specific surface area (BET) is ~12m^2/g. The organic phase includes solvent, plasticizer and a binder. The molecular weight of the binder is 50.000-80.0000 g/mol. Samples with different compositions were created, using the space-filling design of Cornerstone, which is described in Chapter 4.3. The variation ranges of each component is given in Table 1 of the Chapter 4.3. The overview of the derived samples which were prepared are given in Table 2 of the Chapter 4.3. The samples were tested in the sequence of the rheological tests described in the Chapter 4.5.3. The aim of the experiment was to determine the influence of components and their content on rheological values.

6.1. Rheology: Loss factor in Creep and Recovery test

The graph in Figure 14 was derived from the Creep and Recovery test of Profile I. The loss factor value (tan δ) is located on the y-axis, the time in minutes is on the x-axis.

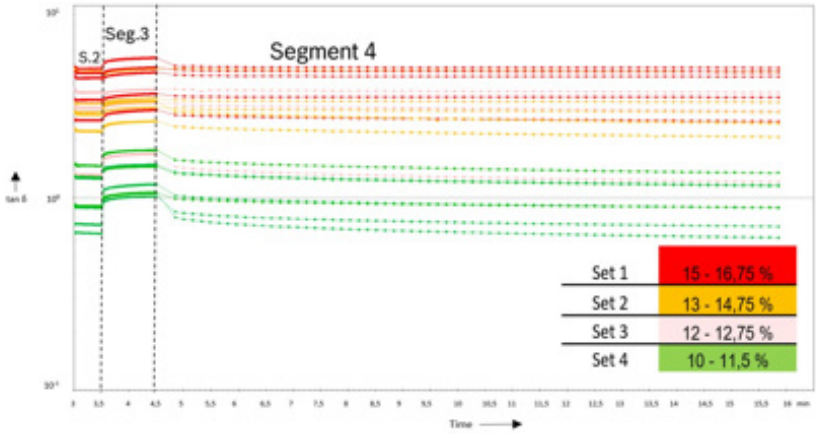

Figure 14. *Loss factor in Creep and Recovery test.*

It can be seen, that the loss factor curves of all pastes vary significantly. Anyway, the samples can be divided in four sets (see Table 5), according to the amount of binder in a system. The red curves represent the samples with the highest binder content between 15 Vol- % and 16, 75 Vol-% (Set 1). The loss factor curves of those samples are considerably high. The orange curves stand for the samples with the binder content of Set 2 (13 -14, 75 Vol- %). Set 3 presents pastes with slightly lower binder content of 12 -12, 75 Vol- %, where samples are shown by the pink curves. The pastes of the Set 4 have the lowest binder content of 10-%-11, 5 Vol- % and relatively low loss factors.

	Binder [Vol-%]	
Set 1	15 - 16,75 %	High binder content
Set 2	13 - 14,75 %	Average binder content
Set 3	12 - 12,75 %	Lower than average
Set 4	10 - 11,5 %	Low binder content

Table 5. *Sets.*

Segment 2 (S2) lays within the time period between 3 and 3, 5 minutes and imitates the sample behavior at rest (applied deformation 0,05%). Followed by Segment 3, where the deformation γ is increased from 0,05 % to 20 % to induce flowing. It is visible, that the loss factor curves of all the samples increase during the process step in different extend. The degree of change of the loss factor values in Segment 3 was evaluated for each sample by extracting the last ten measurement points for the calculation of the mean value. The difference between the mean of the last ten measurement point of the Segment 2 and the mean of the last ten measurement points of the Segment 3 has been calculated in percentage. Pastes of Set 1 demonstrated change in a loss factor in 6 %- 12%, while Set 4 revealed 12 % - 39 %, what indicates improvement in structural strength of the pastes with high binder content. The recovery values of each sample in Segment 4 were also determined. The difference between the mean of last ten measurement points of the Segment 2 and the last ten measurement points of the Segment 4 was calculated in percentage. All samples demonstrated high recovery values between 94 % and 100%.

It can be concluded, that there is a tendency indicated by an increase of the loss factor with increasing binder. All samples of Sets 1 to 4 show viscoelastic behavior. Sets 1-3 belong to viscoelastic liquids (G”>G’ in LVE), while Set 4 shows gel character (G’>G” in LVE).

Generally, the amount of binder influences the degree of change in loss factor in a process step (the higher binder content the lower the change in values). The high recovery values are independent from the binder content.

Influence of the Analyzed Factors On the Loss Factor

Pareto Effect graph has been derived from Cornerstone (Fig.15) to evaluate the influence of the analyzed factors on the loss factor in a Creep (Seg. 3, Figure 14).

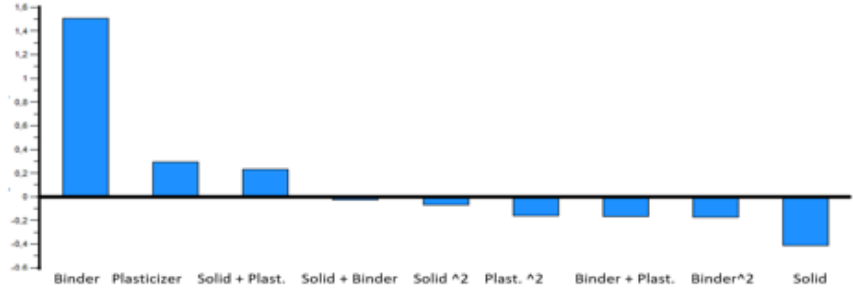

Figure 15. *Influence of the analyzed factors on the loss factor: y-axis represent the loss factor value.*

The biggest influence is given by the binder, as it shows the highest bar. This is another confirmation that the binder increases the loss factor. As can be seen, plasticizer and an interaction of solid + plasticizer contribute to an increase of loss factor, whereas solid squared, binder squared, plasticizer squared and the interaction of binder + plasticizer are minimizing the resulting loss factor.

As just discussed, the terms on their own can influence the rheological parameters, but also by interacting between each other. The graph in Figure 16 demonstrates two terms interaction and shows their impact on the loss factor in a Creep.

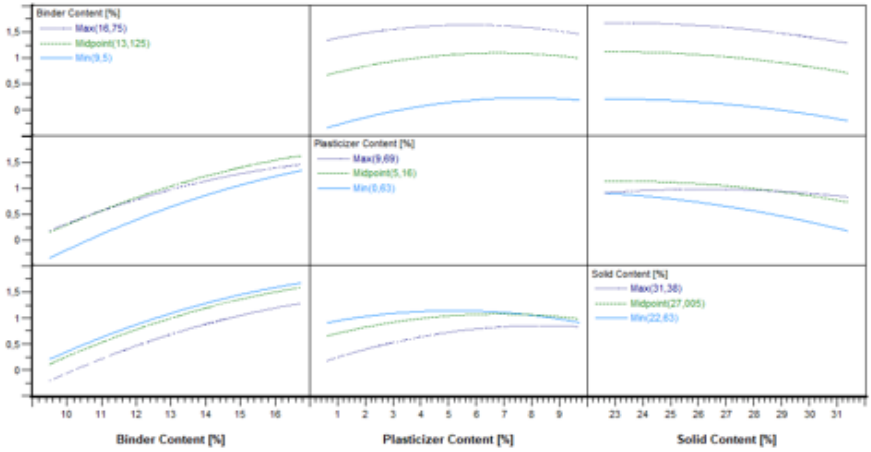

Figure 16. *Interaction graph for loss factor.*

The example, how to read the graph is given in details, starting from the upper row of the interaction graph. The upper square of the left corner represents the dependency of binder content for minimum binder content (9,5 Vol-% - turquoise line), medium binder content (13,125 Vol-% - green line) and maximum binder content (16,75 Vol-% - purple line). The graph on the middle of the upper row shows an increase in loss factor with increasing plasticizer content, whereas the loss factor curve propagation for all three binder contents is comparable. The higher the binder content, the higher the resulting loss factor, as the turquoise curve, which stands for minimum binder content, is the lowest, when the purple one (high binder content)

is on top. The graph on the upper right corner shows that the loss factor curves for all three binder contents are decreasing with increasing solid content.

The middle row shows the dependency of plasticizer content. The graph on the left side of the middle row demonstrates, that the loss factor is increasing with increasing binder content for each plasticizer content. The turquoise line is the lowest, what indicates that the low plasticizer content generates lower loss factors with increasing binder content. At low binder contents, samples with maximum plasticizer content show slightly higher loss factor then the samples with midpoint plasticizer, whereas after the crossover of the two lines in the range of 11 Vol-% binder, the maximum plasticizer containing samples show lower loss factors than those with midpoint of plasticizer content. Such crossover points within a field, indicate the interactions of components, resulting in different curve propagations as shown here. The interactions of the plasticizer and the solid content are given on graph on the right side of the middle row. It can be seen, that the loss factor is decreasing with increasing solid content for the samples with minimum plasticizer content and slightly decreasing for the samples with midpoint of plasticizer content. The samples with the high plasticizer content show almost no change in loss factor with increasing solid content. Crossover point of the samples with the minimum and maximum plasticizer content appears in the range of 23 Vol-% solid. Second crossover point is in the range of 29 Vol-% solid, where the samples with the maximum and midpoint of the plasticizer content show the same loss factor values.

The bottom row illustrates the dependency of the solid content. Graph on the left side of the bottom row shows the same curve propagation - an increase of the loss factor with the increasing binder content - for minimum, average and maximum solid content. The purple line is the lowest compared with the green and turquoise, what indicates that the loss factor of the samples with maximum solid content is decreased. On the graph in the middle, the interaction of the solid and plasticizer is given. The loss factor of the samples with maximum and average plasticizer content increases with increasing solid content, while the samples with the minimum plasticizer content experience quadratic dependency of the loss factor. Therefore, the interaction of the components takes place, as the curves of minimum and midpoint solid content intersect.

Consequently, for an increase in loss factor, binder content should be increased, as it is the most effective influence factor (steepest slope) and/or solid content should be decreased. Plasticizer influence is more or less neglectable. To achieve a lower loss factor, solid must be increased, binder and plasticizer reduced. Although, due to interactions of the samples this dependency

does not always hold. As an example for interactions: at a solid content of 23 Vol-%, samples with minimum and maximum plasticizer content generate the same loss factor value.

6.2. Rheology: Complex Viscosity and Loss Factor In Amplitude-Sweep Test

Amplitude-Sweep test was carried out within the deformation range γ of 0,001-20% with the constant frequency of 1Hz. The analyzed parameters are loss factor (tanδ) and complex
viscosity |η*|.

Loss factor in Amplitude-Sweep test

The results of an Amplitude-Sweep test are shown in a Figure 17, where loss factor (tanδ) is plotted on the y-axis and the deformation γ is on the x-axis. The same sets as in the previous test are used to represent the dependency. The influence of binder on the loss factor can clearly be seen: the higher the binder content, the higher the loss factor. In addition, the pastes with the high binder content have a broader LVE range (see Chapter 4.5.2.), while samples from the Set 4 demonstrate structural breakdown at the lower deformation range. It shows that the binder increases particle network strength within the pastes.

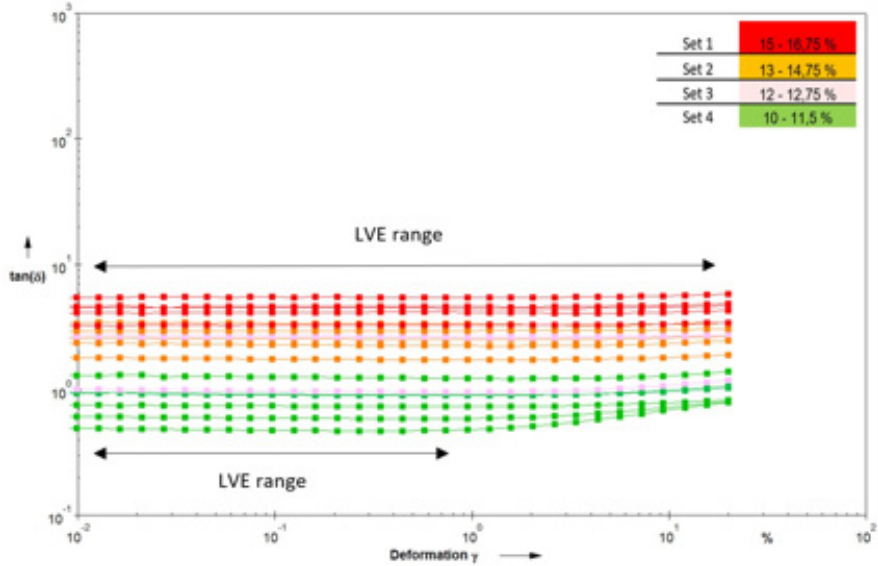

Figure 17. *Loss factor in Amplitude-Sweep test.*

Complex Viscosity In Amplitude-Sweep Test

Different phenomenon is shown by the complex viscosity in an Amplitude-Sweep test, where the solid content instead of the binder content has a primary influence on the complex viscosity. Therefore, samples were divided in three sets (see Table 6), referring to the amount of solid content in a system.

	Solid [Vol-%]	
Set 1	28,25 - 31,38%	High binder content
Set 2	25,44 - 27,63 %	Average binder content
Set 3	22,63 - 24,5 %	Lower than average

Table 6. *Sets according to the solid content in a system.*

Graph in the Figure 18 shows complex viscosity |η*|plotted on the y-axis over the deformation γ on the y-axis. Samples with the low solid content (green curves) experience lower complex viscosity compared with the samples of high (red curves) and average (orange curves) solid content.

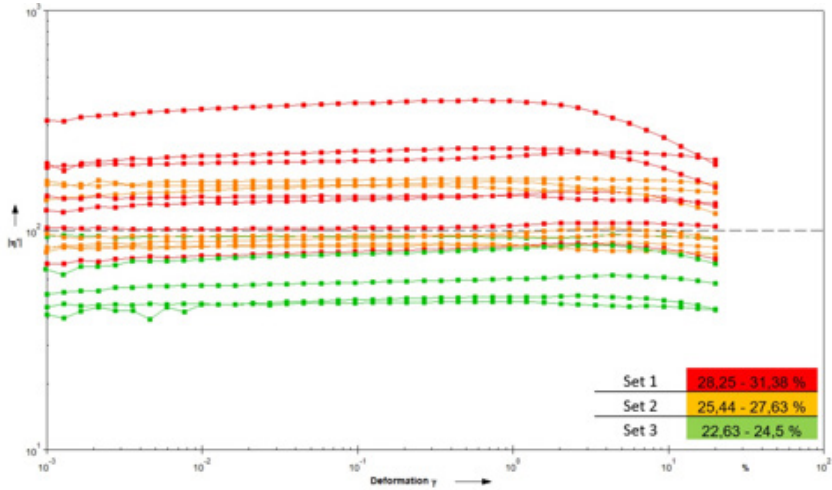

Figure 18. *Complex Viscosity in an Amplitude-Sweep*

The main influence factors for loss factor and complex viscosity are different, revealing that no direct correlation of loss factor and complex viscosity can be expected.

In dependence of the needed rheology, influence factors are revealed. Highest impact on the loss factor is shown by the binder content (the higher the binder content, the bigger the loss factor), while the complex viscosity is more influenced by the solid content (the higher the solid content, the bigger the loss factor).

6.3. Rheology: Complex Viscosity and Loss Factor In Frequency-Sweep Test

Frequency-Sweep test was carried out within the angular frequency ω range of 0,1 - 100 Hz with the constant deformation rate γ of 0,05%. The analyzed parameters are loss factor (tan δ) and complex viscosity |η*|.

Loss Factor In Frequency-Sweep Test

Figure 19 represents the results of the frequency sweep test, where the loss factor over the angular frequency in rad/ s is shown. Colors of the curves represent the amount of binder in a system referring to the sets presented in the Table 5 of a chapter 4.6.1. Two dotted vertical lines on the graph mark extracted values at angular frequencies 1 and 75. The evaluation of those extracted values will be discussed later in this chapter.

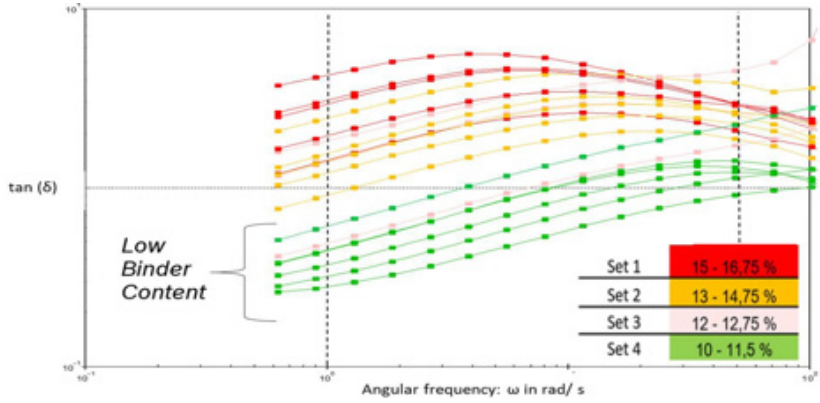

Figure 19. *Frequency sweep test: loss factor.*

All samples show more viscous behavior at angular frequency 100 as the loss factor values at this range are above 1. Although, all the pastes with low binder content (green curves) experience

the transition from more elastic (tan $\delta < 1$) state to more viscous (tan $\delta > 1$) with increasing angular frequency. Meanwhile, pastes from Set 1 stay in the region above 1 over the whole range of frequency change. Samples of the Sets 1 and 2 have a tendency to quadratic dependency of the loss factor with increasing frequency.

Loss factor at angular frequency 1

The effect of the variables on the loss factor at angular frequency 1 and 75 was investigated.

The Pareto Effect graphs in Figure 20 reveals a big influence of the binder on the loss factor at angular frequency 1, which is represented by the highest bar on the left side of the graph. Plasticizer also increases the loss factor, but plasticizer squared minimizes the loss factor in almost the same order. Solid decreases the loss factor (bar on the right side is below zero) as well as an interaction of binder + solid (second bar from the right side).

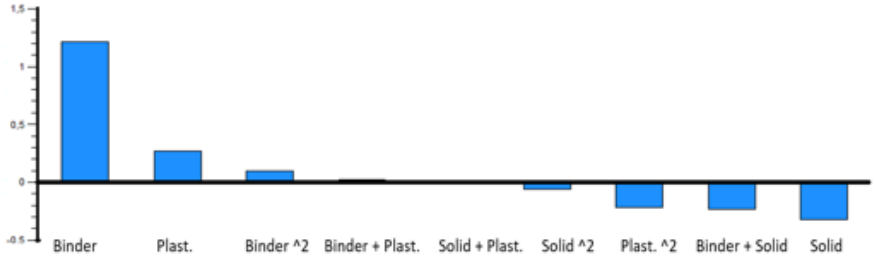

Figure 20. *Influence of the terms on the loss factor at angular frequency 1; y-axis represents the loss factor.*

It is noticeable from the Pareto Effect graph (Fig.20), that the interactions of the binder and solid with the plasticizer have no influence (bars in the middle of the graph under the names "binder + plasticizer" and "solid + plasticizer" are missing). To have more clear vision on interactions of terms, the additional graph in the Figure 21 has been derived from Cornerstone.

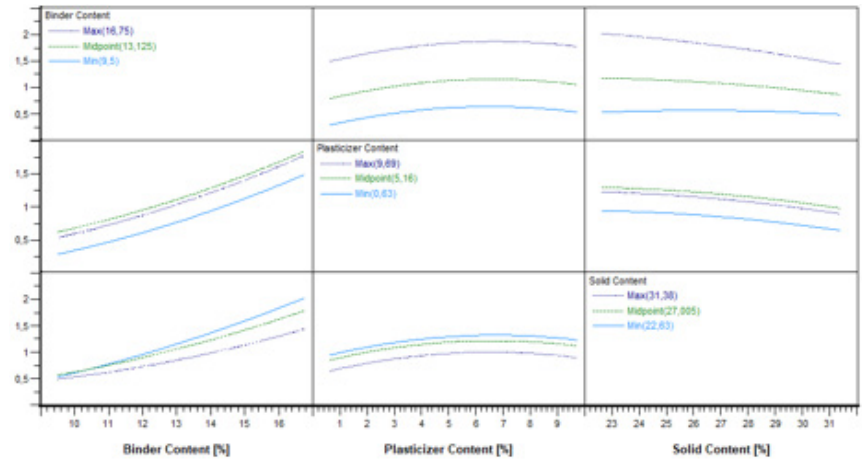

Figure 21. *Interaction graph, loss factor.*

In the upper row the influence of the max, midpoint and max binder content is shown with increasing plasticizer content in the middle graph and increasing solid content in the right graph. With increasing plasticizer, only small or almost negligible increase in a loss factor is noticed for all binder contents (middle graph, upper row). With increasing solid content, loss factor is decreasing for max and midpoint of binder content. Samples with min binder content do not experience change in a loss factor with increasing solid content (right graph, upper row) .It can be seen in Figure 21, that almost no interactions occur and almost all curve propagation show the same dependencies – except interaction of binder and solid content. Therefore different curve propagations are given, revealing a crossover point at low binder contents for minimum and midpoint solid content.

Loss Factor at Angular Frequency 75

As for the loss factor at the angular frequency 75, the biggest influence is also given by the binder. That can been seen in the Figure 22. Plasticizer is another influential parameter and it increases the loss factor at angular frequency 75 in a larger extend then at angular frequency 1 (bar of plasticizer in the Figure 22 is higher than that in the Figure 20). Binder increases the loss factor and binder squared decreases the loss factor (the bar on the right side in the Figure 22). That explains the quadratic dependency of the loss factor of the samples with the high binder content presented in Figure 23. Solid decreases the loss factor slightly more at high frequency (second bar from the right in the Fig. 22) than at low frequency (first bar on the right side in the Fig. 20).

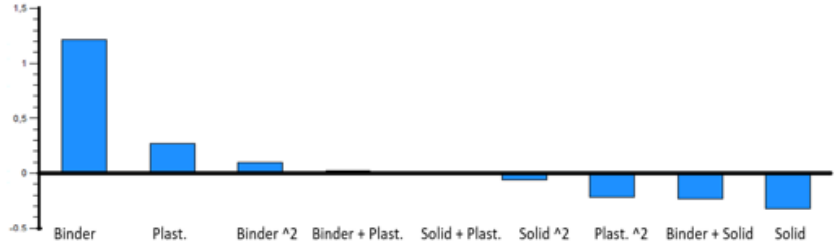

Figure 22. *Influence of the terms on the loss factor at angular frequency 75; y-axis shows the loss factor values.*

As mentioned before, the influence of the terms´ interaction on the loss factor at angular frequency 1 was quite low. In case of angular frequency 75, interactions solid+ plasticizer, binder + plasticizer and binder + solid have bigger influence, what is shown by the bigger bars in Figure 22. Additional information on terms interactions provides the graph in the Figure 23.

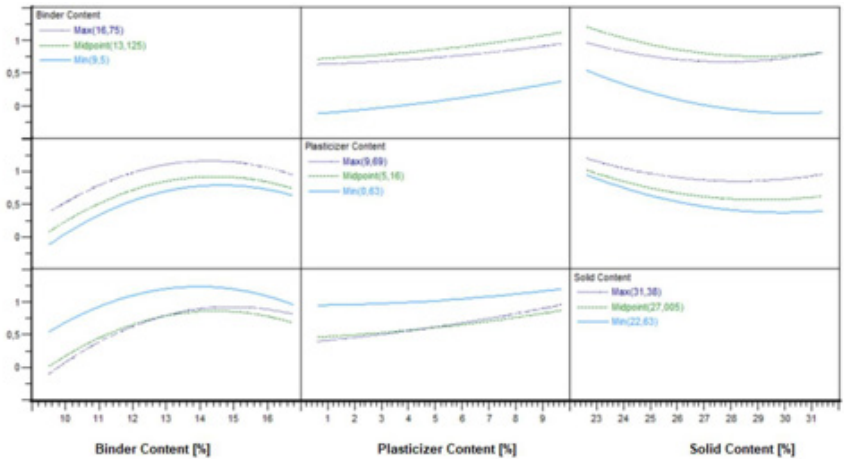

Figure 23. *Interaction graph. Loss factor at angular frequency 75.*

The influence of the binder at its min, midpoint and max is introduced in the upper row of the graph in a Figure 23. In interaction with both – plasticizer (middle graph) and solid (graph on the right), that samples with the midpoint of the binder content (green curve is above all others) have slightly higher loss factor then the samples with the maximum and minimum binder content. Although, when the solid content is around 31% the same loss factor value can be achieved with the max and mid binder content. The combination of minimum binder and maximum solid would reduce the loss factor dramatically as the steepest slope is introduced for min binder content with increasing solid content. Comparable dependencies are shown on the middle and bottom rows. For example, solid at its mid and max point generate almost the same loss factor with increasing binder and plasticizer content.

Consequently, the influential terms change, depending on the angular frequency. Constant influential term in both cases is the binder, which increases the loss factor. Although, quadratic dependency of the loss factor is noticed at high binder content at the angular frequency 75 (Fig 23. left column). Solid decreases the loss factor at both frequencies. Although, quadratic influence of the loss factor of the samples with high solid content at the angular frequency 75 is present (Fig.23 right column). Besides, influence of the plasticizer on the loss factor is frequency dependent. At angular frequency 1, samples with the average plasticizer content show the highest loss factor, while samples at the angular frequency 75 generate the highest loss factor at its maximum point.

Complex Viscosity In Frequency-Sweep Test

Figure 24 represents the result of the frequency sweep test with the complex viscosity, plotted on the y-axis over the angular frequency on the x-axis. Two dotted vertical lines on the graph mark the extracted values at angular frequencies 1 and 75, what will be later discussed in this chapter.

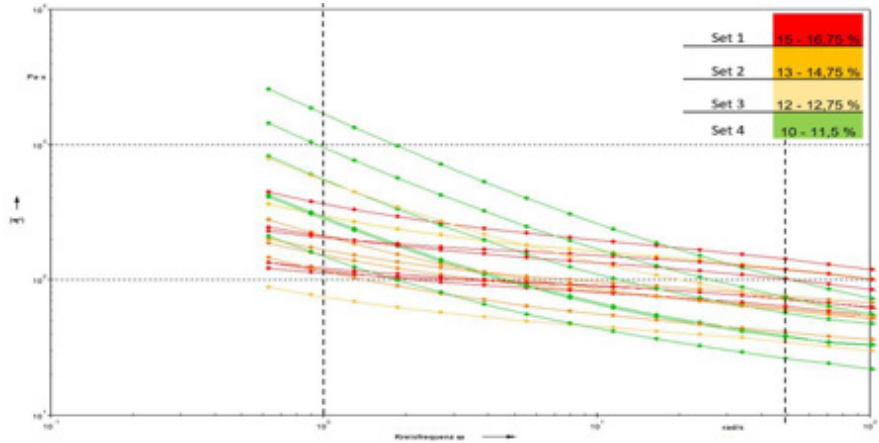

Figure 24. *Frequency sweep, complex viscosity*

It can be clearly seen, that the samples with the higher binder content (red curves) do not experience dramatic decrease in complex viscosity with increasing frequency, but show rather a slight reduction of the values. On the other hand, Set 4 (green curves, low binder content) shows rather rapid decline of complex viscosity values towards higher angular velocities.

Complex Viscosity at the Angular Frequency 1

Pareto Effect graph in Figure 25 reveals the influence of the terms on the complex viscosity at angular frequency 1 rad/s.

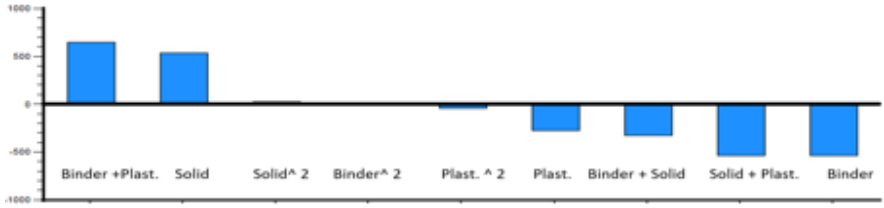

Figure 25. *Influence of the terms on the complex viscosity at angular frequency 1; y-axis shows the complex viscosity value.*

Figure 25 shows, that the binder decreases the complex viscosity (right bar), whereas the interaction of binder + plasticizer increases it and has an important influence (left bar). Solid on its own also increases the value, while solid + plasticizer decreases it. The combination binder + solid slightly lowers the complex viscosity. The squared terms do not have an influence (Solid^2, Binder ^2, Plast. ^2).

Many interactions of the terms are shown on the graph in Figure 26.

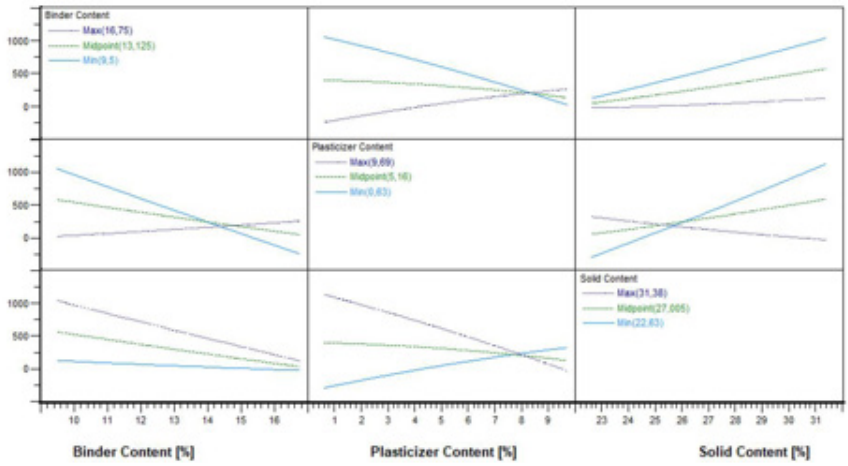

Figure 26. *Interaction graph. Complex viscosity at the angular frequency 1.*

In the upper row, the influence of max, midpoint and min binder content with increasing plasticizer content is shown in the middle graph. For min and midpoint binder content, the complex viscosity is decreasing with increasing plasticizer content. For max binder content, the loss factor is increasing with increasing plasticizer content. As the slopes are different and additionally show different signs, a crossover of all three curves is given. At roundabout 8 Vol-% plasticizer, independent of the binder content, the same complex viscosity can be achieved. In the right graph, the complex viscosity is increasing for all three binder contents with increasing solid content. The resulting slopes for the three binder contents differ also, but a crossover point is not given within the investigations. Probably it will occur at lower solid contents. The biggest impact of solid content is given for min binder, as the slope is the steepest.

In the other rows comparable dependencies are given, as the same components are compared, but based on other origins for min, midpoint and maximum content. In line two, the origin is plasticizer und in line three it is solid content.

Complex viscosity at the angular frequency 75

Pareto Effect graph in the Figure 27 illustrates the influence of the terms on the complex viscosity at angular frequency 75 rad/s.

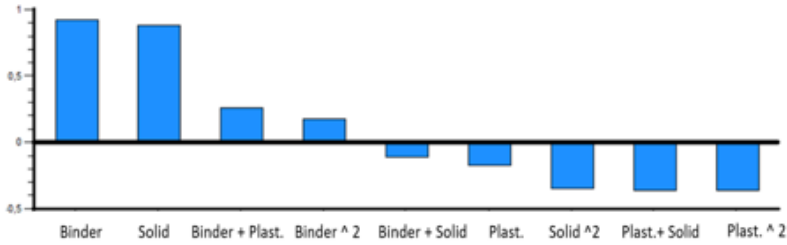

Figure 27. *Influence of the terms on the complex viscosity at angular frequency 75, y-axis shows the square root of complex viscosity value.*

The influential terms for higher frequency are slightly changed. Now along with the binder, solid content has a valuable influence on the complex viscosity. The interaction terms play a smaller role compared with the values in the Figure 25, but still some impact is present: Binder + Plasticizer increase the values, when plasticizer + solid decrease it. Some influence have the squared terms: plasticizer in a power of two decreases the complex viscosity as well as solid^2, binder ^2 increases complex viscosity. The graph below (Fig.28) represents the terms interaction for the complex viscosity at $\omega = 75$.

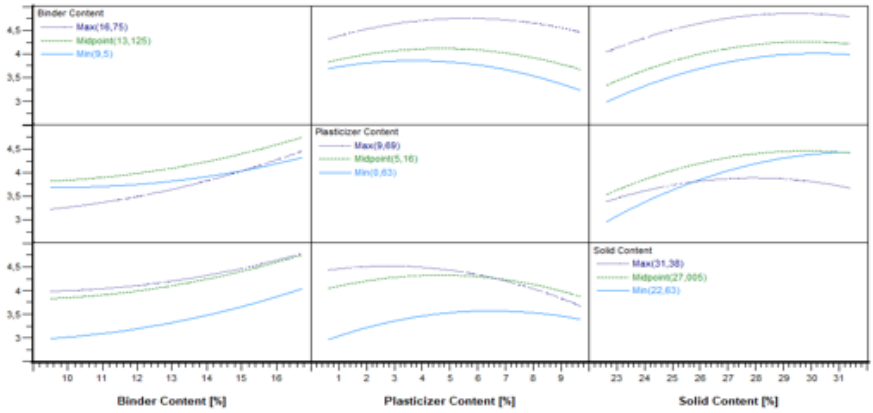

Figure 28. *Interaction graph, complex viscosity at angular frequency 75.*

It can be seen in the upper row that complex viscosity at the frequency 75 increases with increasing solid content for all binder contents (right graph). Quadratic influence of the plasticizer is introduced in middle graph as approximately at plasticizer content of 5-6 Vol-% all curves (min, midpoint and max binder content) increase and slightly decrease towards higher plasticizer content. In the right graph on the upper row, it can be seen that the solid increase complex viscosity at all binder contents. Similar dependencies, but from the perspective of plasticizer and solid are represented by the middle and bottom rows. For example, in the middle graph of the bottom row at the plasticizer content of around 6-7Vol-% solid at its max and midpoint generate the same complex viscosity.

Consequently, at different frequencies, different terms are influential. Binder decreases the complex viscosity at angular frequency 1, whereas increases it at angular frequency 75. Solid increases the values in both cases, but has higher increased influence on the rheological parameter at $\omega = 75$. Plasticizer in interaction with both components - solid and binder - have a big impact on the rheology at $\omega = 1$, and less at $\omega = 75$. At $\omega = 1$ samples with the high solid content experience a decrease in a loss factor with increasing plasticizer content. It is vice versa for samples with the minimum solid content: the loss factor increases with increasing plasticizer content (Figure 26, graph on the middle in the bottom row). Loss factor of the sample with the high binder content increases with increasing plasticizer content, whereas decreases for the

samples with the low binder content with increasing plasticizer content (Figure 26, graph on the middle in the upper row). At $\omega = 75$, plasticizer increases the loss factor at its midpoint in interaction with both components- solid and binder.

Shear Viscosity In Shear Rate Ramp Up Test

In Figures 29, the shear dependent behavior is shown. It can be seen, that all samples represent shear-thinning or pseudo-plastic behavior, which occurs due to disentanglements of the molecular chains of the binder under sufficient amount of force. It allows the chains to orientate in the shear direction reducing the flow resistance [16]. Shear- thinning behavior is one of the requirements for the screen – printing pastes, so that due to the force applied by squeegee, viscosity of the sample is reduced and the paste can flow through the meshes without blocking it.

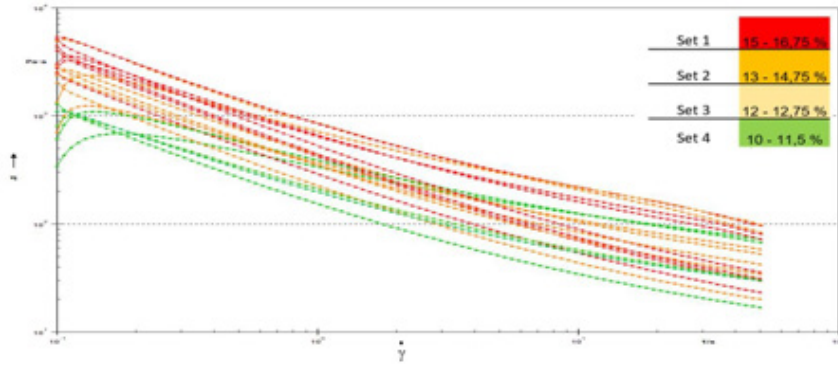

Figure 29. *Shear rate ramp up.*

At low shear rates, an influence of binder content on the sample order is given: the higher the binder content, the higher the viscosity. The shear – thinning behavior with increasing shear rate is different and ends in another order compared to low shear rates, related to interactions with other components.

This dependency is also shown in the Figure 30, where the binder influence is shown by the bar on the left side of the graph. The second and third influential terms are solid content and binder squared. Plasticizer^2 and solid ^2 are the only terms, which decrease the shear viscosity at the shear rate 30.

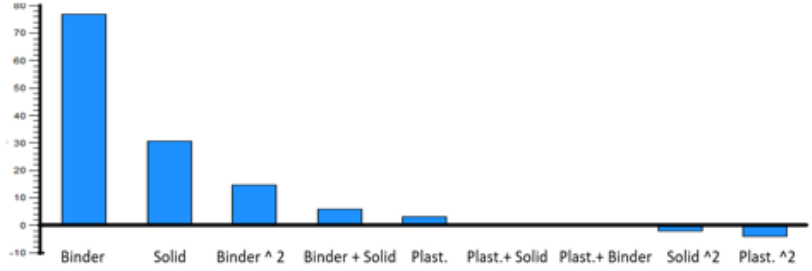

Figure 30. *Influence of the terms on shear viscosity at shear rate 30, x-axis: shear viscosity value.*

Figure 31 shows that binder and solid increase the shear viscosity and no term interaction occurs. Influence of the plasticizer on shear viscosity at shear rate 30 is negligible. That is quite the contrary to the observed results in frequency sweep for the complex viscosity. Therefore different dependencies for rotational and oscillation results concerning viscosity dependencies are given.

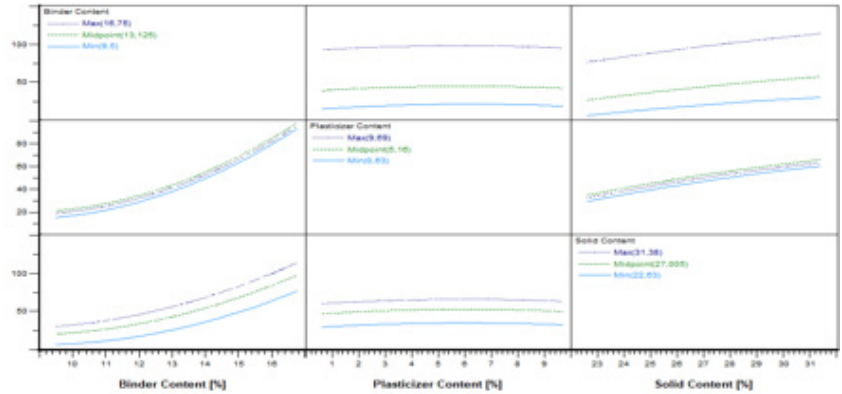

Figure 31. *Interaction graphs. Shear viscosity at shear rate 30.*

Interaction graph for the shear viscosity at the shear rate 50 is introduced in the Figure 32 to show that the terms are influencing the rheology of the samples at the shear rate 30 and 50 almost in the same way.

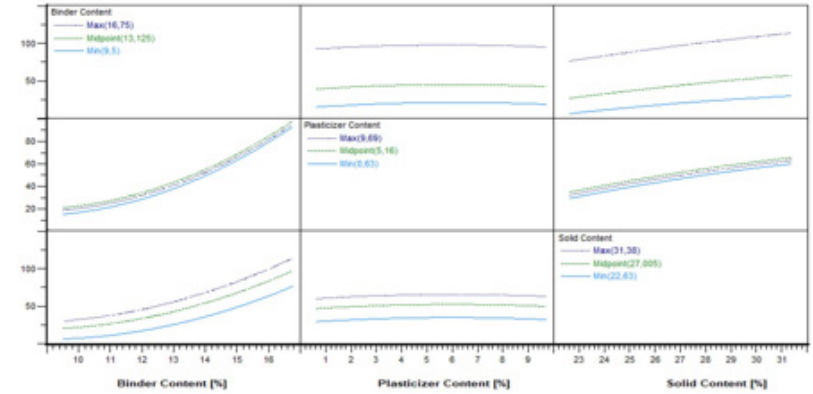

Figure 32. *Interaction graphs. Shear viscosity at shear rate 50.*

To sum up, biggest impact on shear viscosity is given by the binder content as it shows the highest slope, followed by the solid content. With increasing binder and solid content, the shear viscosity will be increased. The plasticizer shows no impact compared to the other two factors.

Term	Loss factor last 10 points	Complex viscosity last 10 points	Viscosity shear rate 30	Viscosity shear rate 50
Constant	0,4197987921	0,33110837983	0,56266861818	0,97079314669
Solid Content	0,63383124119	0,7231788592	0,94304106398	0,70730542957
Binder Content	0,26666766341	0,02147203439	0,06288909465	0,20026799328
Plasticizer Content	0,86179165096	0,10550241932	0,80976789369	0,7730997444
Solid Content^2	0,7426633713	0,4694968809	0,94121078914	0,70778079797
Binder Content * Solid Content	0,21446777565	0,2681479073	0,13423203977	0,4985585931
Plasticizer Content * Solid Content	0,73923472377	0,01202746675	0,95371999552	0,99622038623
Binder Content^2	0,82307873246	0,00652794654	0,02019901704	0,04288396884
Binder Content * Plasticizer Content	0,79428383893	0,11980696365	0,97309474669	0,94438795681
Plasticizer Content^2	0,2551934254	0,72784207704	0,49552789508	0,51120662743
R-Square	**0,951**	**0,9722**	**0,9767**	**0,9721**
Adj R-Square	**0,89591**	**0,940973**	**0,95057**	**0,940627**
RMS Error	**0,452325287**	**9,340961162**	**7,841068282**	**6,378854782**
Residual df	**8**	**8**	**8**	**8**

Figure 33. *Regression table, Profile I.*

Term	sqrt(Loass factor frequency 1)	Log Loss factor frequency 75	Complex viscosity frequency 1	Log Complex viscosity frequency 75
Constant	0,54282099284	0,69497327283	0,67147451957	0,33356090956
Solid Content	0,58882800254	0,39924068169	0,70894848221	0,1873457051
Binder Content	0,65193276785	0,37620516115	0,87649222302	0,85439971269
Plasticizer Content	0,53046583606	0,90826063409	0,44880384463	0,31778745596
Solid Content^2	0,68664806397	0,46203518662	0,93136783627	0,23046067844
Binder Content * Solid Content	0,28073869052	0,61848067222	0,36743238981	0,79282603919
Plasticizer Content * Solid Content	0,94870247318	0,77091497754	0,07269944163	0,27003819343
Binder Content^2	0,52939556923	0,16598501211	0,97531789118	0,57108105589
Binder Content * Plasticizer Content	0,93089752808	0,8406522085	0,04559013829	0,49130625335
Plasticizer Content^2	0,16318822534	0,85515894425	0,84077651757	0,21837881521
R-Square	**0,9374**	**0,7109**	**0,7585**	**0,7655**
Adj R-Square	**0,874877**	**0,421894**	**0,516987**	**0,531084**
RMS Error	**0,158326158**	**0,319007915**	**270,093552**	**0,313343196**
Residual df	**9**	**9**	**9**	**9**

Figure 34. *Regression table, Profile II.*

As a final step, the predicted response graphs (Fig.35, 36) have been derived from the regression tables. The upper and lower lines of each panel indicate the confidence interval; the narrower the lines are, the more accurate the model is. The predicted response graph of profile I represents the more precise model (Fig 35.), while the confidence intervals of the graph of the profile II (Fig. 36) are broader and show more oscillations in the values. The dashed lines, crossing each column, can be moved across the values of the parameters and the influence of each variable on the rheological properties is calculated (see given number on the y-axes). In general, the deeper the slope of a dependency, the higher the importance of this variable on each factor.

6.4. Regression analysis

The reproducibility and reliability of the extracted model, which links the responses and factors, can be evaluated by analyzing the regression tables for both rheology profiles (Fig. 33, 34). Each term is categorized, according to the genuineness of the results. Terms < 0,05 indicate very genuine results, while terms > 0,1 represent the relationship due to chance. R-Square value is dependent on the number of terms in a model, consequently, it increases and decreases by adding new terms and does not always indicate the reliability. Adjusted R- square (Adj R-Square) increases only, if the new term improves and provides better accuracy of the model. Residual df (degree of freedom) refers to the number of data points accessible to estimate the standard deviation of the residuals. To improve the values of the regression table, mathematical transformation of the responses is often needed.

The Adj R-Square values of the Profile I (Fig. 33) reached their maximum values without transformation, while the regression table of Profile II (Fig.34) required modifications: the values of the loss factor at frequency 1 required the rescaling to square root, whereas the loss factor and the complex viscosity at frequency 75 were transferred to a logarithmic scale (Fig. 33 and 34). It can be easily observed, that the values of the Profile I show more reliability then the ones of the Profile II.

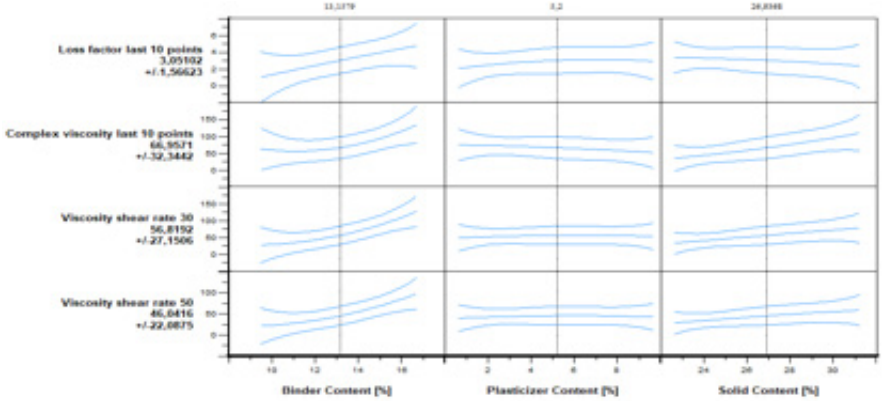

Figure 35. *Predicted response graph, Profile I.*

For figure 35, the following dependencies occurred: with increasing binder content, each analyzed factor (loss factor, complex viscosity and shear viscosity) is increased. Slightly less steepness of the slope is represented by the curves in a column of the solid content. Different behaviors are given here: with increasing solid content, the loss factor of the last ten measurement points is decreased; all other analyzed factors (complex viscosity and shear viscosity) are increased. The plasticizer shows very low or almost negligible influence.

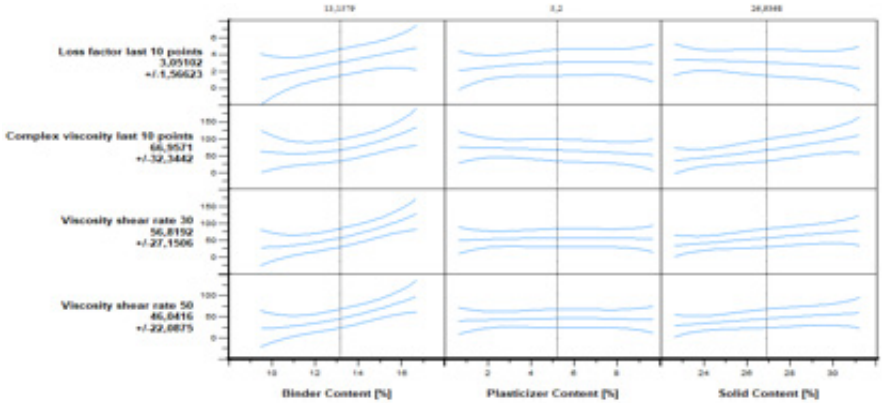

Figure 36. *Predicted response graph, Profile II.*

In figure 36, predicted response graph for the Profile II is present. The model is less accurate as the upper and lower boundaries of the confidence interval are located wider from each other for all the analyzed factors. The following dependencies can be observed: binder (left column of the graphs) increases the loss factor at angular frequency 1 and slightly increases it at angular frequency 75. Complex viscosity at angular frequency 1 is decreasing with the increasing binder content, whereas at angular frequency 75 an opposite tendency occurs. The middle column shows that the influence of the plasticizer on the rheology is very low. Slightly bigger influence arise due to the solid content in a system: solid slightly decreases loss factor and slightly increases complex viscosity.

6.5. Conclusion

The rheology of the pastes is affected the most by the binder content in a system. The second influential parameter is the solid content. Plasticizer only shows minor impact on analyzed parameters. Although, in an interaction with both component-solid and binder some influence of the plasticizer is noticed. The following theses describe the rheology of tested samples in details:

- Samples with the high binder content are more resistant to high shear rates. This phenomenon has been observed during Creep and Recovery test, where samples with the high binder content show less change in rheological parameters in a process step (chapter 4.6.1.) and Amplitude-Sweep test, where wider LVE-range is present for the samples with high binder content (4.6.2). Therefore, if the samples are required to keep structural strength as long as possible over the whole application process, addition of more binding agent would be a solution, and vice versa.

- To increase the loss factor in a process step more binder and/or less solid has to be added in a system (chapter 4.6.1.).

Influential terms may change depending on the frequency applied on the samples:

- If during the printing process, slow motions on a long timescale take place (corresponds to angular frequency 1), high binder content and low solid content would increase the loss factor. In this case, plasticizer also have some influence as it contributes to the loss factor increase.

  If complex viscosity needs to be increased, then more solid must be added in a system and/or less binder. It is important to consider, that the plasticizer in interaction with both terms has strong effect on rheology. Such that, if the solid on its own increases the complex viscosity, in interaction with plasticizer the complex viscosity is decreased (chapter 4.6.3. Figures 25, 26). To avoid unexpected rheology due to strong interactions of the terms

with the plasticizer, the content of the plasticizer in the samples must be around 5 Vol-% (midpoint) (Chapter 4.6.3. Figure 26).

- If during the printing process, fast motions on a short timescale take place (corresponds to angular frequency 75), loss factor is increased by adding average amount of binder (13 Vol-%). At high binder content (16 Vol-%) loss factor slightly decreases quadratically. Decline in a loss factor value also occurs by adding more solid in a system and less plasticizer (Chapter 4.6.3. Figures 22, 23).

  If at low frequency, binder decreases complex viscosity, at high frequency it increases the value. Therefore, complex viscosity will be higher if the amount of binder and solid is increased. If the complex viscosity must be reduced, but the amount of solid should stay the same (for example, if the amount of solid content defines the functionality of the printed layer, therefore cannot be lowered), the then addition of the plasticizer may help as the interaction solid + plasticizer decreases the rheological value. (chapter 4.6.3. Figures 27, 28)

- Shear viscosity (at the shear rate 30 and 50) increases with increasing solid and binder content. Plasticizer, in this case, plays minor or no role in rheology. All samples independent of its composition show shear-thinning behavior.

  Hence, the composition of the pastes must be adjusted based on the required rheology and the printing settings.

7. Influence of the binder and powder type on the rheological values

Rheology of the samples can be influenced not only by the paste composition but also by the type of the components. To evaluate the influence of different powders and binders on the rheological values, two ceramic powders (A and B) and two binders (1 and 2) have been tested. Specific surface area (BET) of the powder A is 10 m^2/g, and that of the powder B is 25 m^2/g. Molecular weight of the binder 1 is 90.000 – 120.000, and that of the binder 2 is 50.000 – 80.000 (Table 7).

Powder	Specific surface area (BET)	Binder	Molecular Weight of the Binder
Powder A	10 m^2/g	Binder 1	90.000 - 120.000 g/mol
Powder B	25 m^2/g	Binder 2	50.000 - 80.000 g/mol

Table 7. *Specifications of powder and binder.*

The ranges of the components are given in a Table 8. As it can be seen, minimum solid content for the powder A is set to 22 Vol-%, and the maximum to 32 Vol-%. For the powder B the range is different (5 – 15 Vol-%), due to higher specific surface area of the powder minimum and maximum values are lower. Therefore, the composition of the compared samples is not the same.

Powder type	Solid [Vol %]	Binder [Vol %]	Plasticizer [Vol %]
A	22–32	9–17	0–10
B	5–15	9–17	0–10

Table 8. *Ranges of the components.*

Four sets have been created so that each powder type is tested with each binder (Table 9). Set contains powder A and binder 1; Set 2 contains powder A and binder 2; Set 3 contains powder B and binder 1 and Set 4 contains powder B and binder 2. Each set contains 19 samples, so that in total 76 samples were created and analyzed.

A1	Set 1
A2	Set 2
B1	Set 3
B2	Set 4

Table 9. *Sets.*

After the calculation of the different samples, all pastes were prepared as described in chapter 4.4. Two rheology profiles (shown in a chapter 4.5.3) were used to analyze the samples.

In the following part not each DoE-result is discussed on it's own as it was done in chapter 4.6 The resulting ranges of each set, which were achieved for viscosity (at shear rate 50 [1/s]) and loss factor (extracted at angular frequency 1 [1/s]), are compared to show the influence of powder and binder types.

Shear Viscosity In a Shear Rate Ramp Up Test

The ranges of shear viscosity at the shear rate 50 are compared in Figure 37.

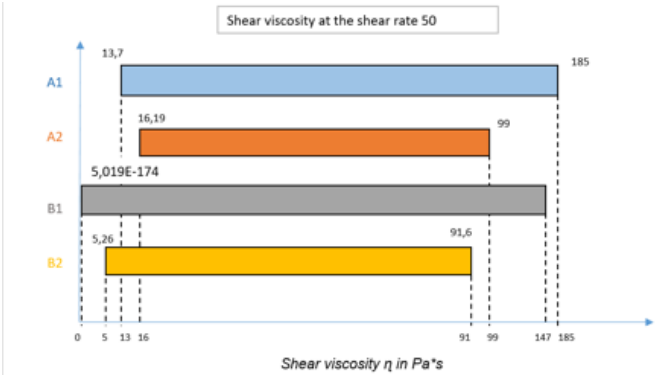

Figure 37. *Comparison of the sets. Shear viscosity at the shear rate 50.*

As it can be seen, Set B1 has the widest viscosity range, followed by set A1. Sets A1 and B1 generate high viscosity with the maximums at 185 Pa*s and 147 Pa*s accordingly. In both of the Sets, binder 1 is used, which has high molecular weigh (90.000 - 120.000 g/mol). Molecular weight of binders is determined by length of molecular chains and degree of chain entanglement [5]. Therefore, increased molecular weight causes the enhancement of intermolecular attractions leading to higher flow resistance and increased viscosity.

The Sets A2 and B2 present narrower viscosity range and lower maximum viscosity can be achieved, presumably, due to lower molecular weight of the binder 2.

Hence, it can be concluded, that the binder type has more influence on the shear viscosity at the shear rate 50 than the powder type, as the Sets with the same binder type but different powder type show similar tendencies.

Loss Factor In a Frequency-Sweep Test

Figure 38 shows the ranges of the loss factor for each set at angular frequency 1.

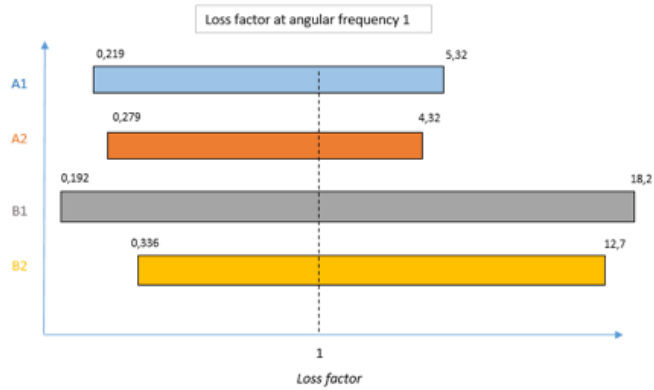

Figure 38. *Comparison of the sets. Viscoelastic behavior.*

All sets reveal viscoelastic behavior. It can be observed, that the set B1 generates a wide range of the loss factor reaching minimum and maximum values among the sets. Set B2 also has a high maximum loss factor value, what tells us about predominant viscous behavior of the pastes. Smaller loss factor values and narrower ranges are shown by the sets A1 and A2 compared to sets B1 and B2. Therefore, it can be concluded that the loss factor is mostly affected by the powder type and content rather than by the binder type as the sets with the same powder and different binder show similar tendencies.

7.1. Conclusion

Influence of the powder A and B:

- Powder A generates narrower range of the loss factor at angular frequency 1 than the powder B due to the higher solid content. Comparison of the samples of powder A and powder B with similar composition can be seen in the Table 10 (ranges of solid content are different for powders A and B due to different BET). The powder B generates higher viscosity at the shear rate 1 for most of the pastes and a lower loss factor at the angular frequency 1. The samples with the low solid content (22-Vol% for powder A and 5-Vol% for powder B) are exceptional as the pastes with the powder B generate higher loss factor and lower viscosity.

Paste		Solid		Binder	Plasticizer	Loss factor (angular frequency 1)		Shear Viscosity (shear rate 1)		Shear Viscosity (shear rate 50)	
Powder A	Powder B	Powder A	Powder B			Powder A	Powder B	Powder A	Powder B	Powder A	Powder B
P578	P643	22	5	14,33	3,33	4,14	11,2	292	37,3	60,7	26,7
P582	P638	25,33	8,33	11,67	0	1,85	1,28	149	301	67,4	44,9
P577	P640	28,67	11,67	11,67	10	1,7	0,72	650	608	65,9	48,7
P586	P627	28,67	11,67	14,33	0	1,99	0,592	957	3060	103	3,64268E-68
P594	P637	32	15	9	10	0,412	0,192	658	2390	84,8	61,9
P576	P636	32	15	14,33	6,67	1,78	0,294	1240	4420	108	132

Table 10. *Comparison of the samples with different powders.*

  Therefore, the BET is dominant. The higher the BET, the higher the expected viscosity and the lower the expected loss factor. Although, at the shear rate 50, this dependency does not hold as the viscosity of samples with the powder B is lower than that of the powder A. It can be explained by stronger shear-thinning behaviors of the samples with the powder B.

- Minimum loss factor values achieved with the powder A: 0,219 (A1) and 0,279 (A2). Maximum loss factor values: 5,32 (A1) and 4,32 (A2). Samples with powders B have wider range of the loss factor. Minimum loss factor values achieved with the powder B: 0,192 (A1) and 0,336 (A2). Maximum loss factor values: 18,2 (A1) and 12,7 (A2).

Different dependency is recognized for the shear viscosity, where binder type has more influence than the powder type. Influence of the binder 1 and 2:

- Samples with the binder 1 generate higher viscosity than the samples with the binder 2 independent of the used powder. The maximum shear viscosity achieved with the binder 1: 185 Pa*s (A1) and 147 Pa*s (B1). The minimum: 13,7 Pa*s (A1) and 5,019E-174 Pa*s (B1).

- Lower shear viscosity is demonstrated by the samples with the binder 2. Maximum: 99 Pa*s (A2) and 91,6 Pa*s (B2). Minimum: 16,9 Pa*s (A2) and 5,26 Pa*s (B2).

Therefore, if the lower shear viscosity at the shear rate 50 is needed then the binder 2 would be a solution. Although, the combination of binder B and powder 1 also shows low viscosity for the

samples with low powder content as the minimum possible viscosity is approaching zero. In general, the Set B1 presents the widest ranges of shear viscosity and loss factor. Consequently, if the narrower ranges are required, combination of binder 1 and powder B should be avoided.

Hence, the shear viscosity is mainly influenced by the binder type and its molecular weight rather than by the powder type. Whereas powder type and therefore BET of the solid content has bigger impact on the loss factor. This dependency holds only for these particular powders and binders. Changing components would lead to different rheology values and, possibly, different dependencies could be found.

8. Sources

[1] Mahendra R.Somalu, Andanastuti Muchtar, Wan Ramli Wan Duad. Nigel P. Brandon, 2016, Screen-printing ink for the fabrication of solid oxide fuel cell films: a review.

[2] Debora Marani, Christophe Gadea, Johan Hjelm, Per Hjalmarsson, Marie Wandel, Ragnar Kiebach, 2014. Influnence of hydroxyl content binders on rheological properties of cerium-gadolinium oxide (CGO) screen printing inks

[3] M.R. Somalu, V. Yufit, N.P. Brandon, 2012. The effect of solids loading on the screen-printing and properties of nickel/scandia-stabilized-zirconia anodes for solid oxide fuel cells

[4] Dr. Theo Wember. Design of Experiment (DoE) Systematic and efficient development of products and processes and empirical model building based on statistical principles, Version 1.4

[5] Tatsuki Ohji, Mrityunjay Singh, Sanjay Mathar. 2014, Advanced Processing and Manufacturing Technologies for Nanostructures and Multifunctional Materials, *Ceramic Engineering and Science proceeding*

[6] Hoornstra, J., Weeber, A.W., de Moor, H.H.C.. Sinke, W.C.,1997, The Importance of Paste Rheology in Improving Fine Line, Thick Film Screen Printing of Front Side Metallization; Netherlands Energy Research Foundation ECN: Petten

[7] Olagoke Olabisi, Kolapo Adewale, 2015. *Handbook of Thermoplastics*

[8] Łucja Dybowska-Sarapuk, Jerzy Szalapak, Grzegorz Wróblewski Małgorzata Jakubowska, 2016, Rheology of inks for various techniques of printed electronics, Warsaw University of Technology

[9] Hongming Li, 2002, Impact of cohesion forces on particle mixing and segregation, University of Pittsburgh

[10] Kuide Qin, Abbas A Zaman, 2003, Viscosity of concentrated colloidal suspensions: comparison of disperse models, *Journal of Colloid and Interface Science. Volume 266, Issue 2*, 15 October 2003, Pages 461-467

[11] Michael Scott Eldred and Steven F. Wojtkiewicz , 2013, Overview of modern design of experiments methods for computational simulations, American Institute of Aeronautics and Astronautics

[12] Sebastian Burhenne, Dirk Jacob, and Gregor P. Henze, 2011, Sampling based on Sobol' sequences for Monte Carlo techniques applied to building simulations, Fraunhofer Institute for Solar Energy Systems, Freiburg, Germany and University of Colorado, Boulder, USA

[13] Thammarat Thamma, Jaratsri Rungrattanaubol and Anamai Naudom, 2014, Modification on Search Algorithm for Computer Simulated Experiment

[14] Goodwin, Hughes, 2008. *Rheology for Chemists. An Introduction*

[15] Dr. Hans M. WyssRyan J. Larsen, Prof. David A., 2007, Oscillatory Rheology Measuring the Viscoelastic Behaviour of Soft Materials Weitz Harvard University Physics & DeAS Cambridge, USA, *G.I.T. Laboratory Journal 3-4/2007*, pp 68-70.

[16] Thomas G. Mezger, 2015. *Applied Rheology*.

[17] Thomas G. Mezger, 2002. *The Rheology- Handbook*.

[18] Sefar, 1999. *Handbook of Screen-printing*.